



THE UNIVERSITY *of* EDINBURGH

Edinburgh Research Explorer

Measurement of gaseous hydrocarbon distribution by a near-infrared absorption tomography system

Citation for published version:

Hindle, FP & McCann, H 2001, 'Measurement of gaseous hydrocarbon distribution by a near-infrared absorption tomography system', *Journal of Electronic Imaging*, vol. 10, no. 3, pp. 593.
<https://doi.org/10.1117/1.1377306>

Digital Object Identifier (DOI):

[10.1117/1.1377306](https://doi.org/10.1117/1.1377306)

Link:

[Link to publication record in Edinburgh Research Explorer](#)

Document Version:

Peer reviewed version

Published In:

Journal of Electronic Imaging

General rights

Copyright for the publications made accessible via the Edinburgh Research Explorer is retained by the author(s) and / or other copyright owners and it is a condition of accessing these publications that users recognise and abide by the legal requirements associated with these rights.

Take down policy

The University of Edinburgh has made every reasonable effort to ensure that Edinburgh Research Explorer content complies with UK legislation. If you believe that the public display of this file breaches copyright please contact openaccess@ed.ac.uk providing details, and we will remove access to the work immediately and investigate your claim.



Measurement of gaseous hydrocarbon distribution by a Near Infra-Red absorption tomography system

F. P. Hindle^a, S.J. Carey^a, K.B. Ozanyan^a, D.E. Winterbone^b, E. Clough^b, and H. McCann^a

^aDept. of Electrical Engineering & Electronics,

^bDept. of Mechanical Engineering,

UMIST, PO Box 88, Manchester M60 1QD, UK.

ABSTRACT

The spatial distribution of chemical species can be a critical determinant of chemical reactor performance. The spatial variation of air-fuel ratio in a combustion chamber of an Internal Combustion engine has significant influence on fuel efficiency and emissions. We report the development of a fibre-based Near Infra-Red Absorption Tomography system, to measure the distribution of hydrocarbons in-cylinder. It has been successfully applied to transient gas injections. The technique exploits the specific (but weak) hydrocarbon absorption of 1.7 μm radiation, which wavelength has only recently become accessible by availability of solid-state all-optoelectronic components. A standard telecommunications laser was also deployed to measure reference information. The measurement space is sampled by 32 dual-wavelength fibre-coupled measurement paths. The logarithm of the ratio of the two measurements yields the path integral of the hydrocarbon absorption, and hence, of concentration. The path integral is measured with typically 28dB signal-to-noise ratio (SNR). Single-channel characterisation shows that the technique is readily calibrated for temperature and pressure effects, over the region 70–150°C and 1-10bar. Tomographic reconstruction of different gaseous hydrocarbon flows has been achieved with spatial resolution of the order $D/5$, where D is the vessel diameter. Temporal resolution of about 1,000 frames per second is demonstrated.

Keywords : Tomography, Infra-red, absorption, system, hydrocarbon, gas, measurements

1. INTRODUCTION

The behaviour and performance of chemical reactors depend on many parameters such as temperature, pressure and the relative spatial distributions of the reactants. In many cases, the last of these can be dominant, so the optimisation of the distribution of chemical species can determine the success, or limitations, of many commercial processes. Hence, equipment designers could utilise a technique to measure (or ‘image’) such distributions for the purpose of design optimisation. It is also clear that such species imaging could be used in the control of the process, if robust instrumentation were available which complied with the various control needs such as temporal and spatial resolution. Electrical tomography is under rapid development for cases where there is a contrast of bulk electrical properties between reactants, typically where the reactants are in different thermodynamic phases, but sometimes also when they are both liquids¹. In many cases, however, there is insufficient electrical contrast between reactants; this is generally true when the reactants are all in the gas phase. Dopant-based techniques have enjoyed success for some cases, such as solid particulate tracking by Positron Emission Tomography² where a β^+ -emitting radionuclide “label” is incorporated in some of the particles; another example is gas-gas mixture imaging after introducing a fluorophore (see section 1.1 below).

In this paper, we present the first image data obtained from an All-Opto-Electronic (AOE) Near Infra-Red (NIR) absorption tomography system which is designed to measure the 2-dimensional distribution of gaseous hydrocarbon (HC) species mixing with air. It is intended to apply such a system to research and development in internal combustion (IC) automotive engines. This system provides direct HC imaging capability, without the use of dopants. In a previous paper³, we have presented the principles and some design features of the system, along with feasibility tests of single-channel performance, with a monochromator source.

1.1. HC imaging in IC engines

The need for in-cylinder HC vapour imaging in automotive engine R&D has arisen from the commercial and environmental imperatives to improve fuel economy and reduce harmful emissions to the atmosphere⁴. The predominant technique used to date for this purpose is Planar Laser-Induced Fluorescence (PLIF), with a range of fluorophore dopants; 3-pentanone is favoured by many workers⁵ for its excellent thermodynamic match with iso-octane (the standard test fuel used for automotive engine R&D) and its convenient fluorescence stability with respect to temperature and pressure variations and oxygen presence. Nevertheless, PLIF has many limitations: firstly, the use of a dopant means that the technique is fundamentally “indirect”, in that one monitors the dopant concentration rather than that of the fuel, and is ultimately constraining, e.g. making the study of multi-component fuels difficult; secondly, large-scale optical access is needed in two orthogonal planes in order to get the stimulating laser sheet into the cylinder and to image the fluorescence with an array imaging detector; thirdly, the image framing rate of the technique is limited by the pulsing characteristics of the high-energy pulsed lasers used, and is typically poorer than 100Hz⁶, making it impossible to follow the flow within a single engine cycle. Despite these limitations, PLIF is widely used⁷ and some of us are engaged in attempts to overcome the latter two areas of limitation by using a tomographic fluorescence technique which exploits emergent UV laser diode devices⁸.

1.2. Near-IR absorption tomography

IR absorption tomography has the potential to overcome all of the above limitations : it can be made to image HC species without the use of dopants; an array of optical fibres in a single plane can be used instead of large glass inserts; and relatively fast signal measurements (> 10kHz) are easily attainable. The use of optical fibres in engines has been developed by several authors⁹⁻¹¹ for a wide range of both combustion and lubrication studies, exploiting a wide range of wavelengths. However, the critical enabling feature of the present study is the emerging commercial availability of IR laser diode sources, which could eventually cover a wide range of wavelengths with suitable power delivery at room temperature.

The basic principle of the sensing technique is the measurement of attenuation of a pencil beam of monochromatic IR light due to rotational/vibrational absorption by a particular molecular species. The attenuation process is described by the Beer-Lambert law:

$$I_r(\lambda) = I_o(\lambda)e^{-k(\lambda)cl} \quad (1)$$

where

$I_r(\lambda)$ = received light intensity at wavelength λ after traversing a distance l

$I_o(\lambda)$ = launched light intensity at λ

$k(\lambda)$ = absorption coefficient at λ

c = molar concentration.

In practice, other non-specific attenuation mechanisms will apply, such as the passage of particles through the beam, light scattering by transparent fuel droplets, or refractive index variations due to temperature inhomogeneities. Hence, a further wavelength is deployed as a reference, which is insensitive to the target chemical species, but subject to the same non-specific attenuation mechanisms as the resonantly absorbed wavelength. To ensure accurate hydrocarbon concentration measurements the wavelength separation of the measurement and reference lasers must be sufficiently small to neglect the differences expected in the responses to this interference. Such a dual wavelength system should be able to accurately measure hydrocarbon concentrations in a running engine, where soot particles and fuel droplets will be present in the measurement path. Ideally, beams at both wavelengths are passed along the same path through the subject simultaneously. In that case, the light received by the detector is given by :

$$I_r = I_o(\lambda_1) \cdot \exp\left(-\int_L k(\lambda_1)c(x,y)dl\right)F + I_o(\lambda_2) \cdot \exp\left(-\int_L k(\lambda_2)c(x,y)dl\right)F + I_{TL} \quad (2)$$

where F expresses the non-specific attenuation and I_{TL} is the intensity due to black-body radiation of surfaces in the detector's field of view. To enable an image of the concentration distribution to be reconstructed, a tomographic system requires the use of multiple beam paths through the subject, at different orientations. High temporal resolution (for a rapidly changing measurement subject) requires all orientations to be sampled simultaneously.

As discussed previously³, several IR wavelengths are of use for HC absorption measurement. Previous authors with interests in IC engine studies have attempted^{12,13} to use the fundamental C-H stretch absorption at 3.4 μm , and the much less strongly absorbed 2.3 μm ¹⁴. In both cases, however, the source and detector technologies used were such as to prevent the development of systems with multiple simultaneous paths, each carrying multiple IR wavelengths. We believe the system we present here is unique to date in achieving this combination for an IR tomography system operating by absorption measurements alone. By selecting absorption of the 1700 nm wavelength³ (the overtone of the fundamental C-H vibration at 3.4 μm), we have been able to deploy commercially available laser diodes, optical components, and IR detectors to measure HC concentration in a system which is amenable to extension to large numbers of simultaneous absorption paths of multiple wavelengths, under AOE control, and hence to tomographic reconstruction.

2. THE NIR TOMOGRAPHY SYSTEM

2.1. Layout

Figure 1 shows the physical layout of the 32 beam paths in the present system, as they pass through an 85 mm inner diameter chamber which mimics the combustion chamber of an IC engine. For engineering simplicity at this stage, optical access to the chamber was through a glass “slice” manufactured from fused silica of thickness 11.5mm, of the type often used for engine studies¹².

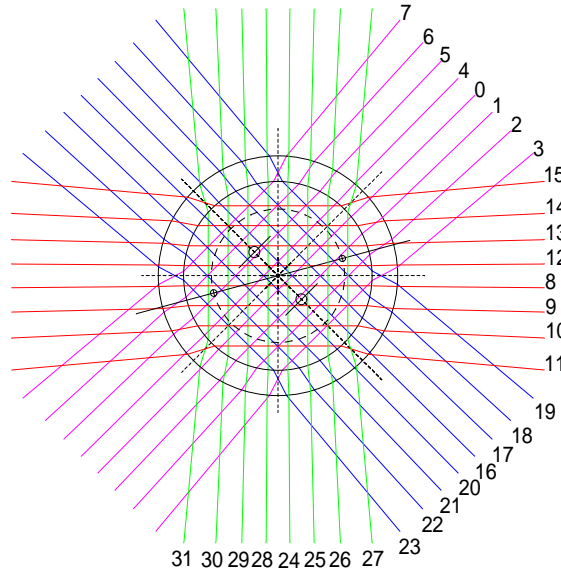


Figure 1 The optical beam paths in the 32-channel system, glass ring shown

The 1700 nm source is a DFB InGaAsP laser diode (of linewidth 1.5MHz), custom-built to our specification, delivering 3mW in CW mode. Thermoelectric control provides tunability over approx. 1nm. All measurement data reported here were obtained at 1699.9nm, except where otherwise indicated. Over the tunable range, no significant variation of absorption was observed in stoichiometric iso-octane/air mixtures. The reference wavelength source is a 1550 nm communications laser diode (kindly donated by Nortel), providing 2mW CW.

The diode laser outputs are coupled into a standard telecoms single-mode fibre by a custom-built fused biconical taper wavelength division multiplexer (SIFAM). The light is then fanned out to 32 fibres by a 1x32 integrated optic coupler (PIRI), as shown in the optical circuit in Figure 2. Graded index lenses (Nippon Sheet Glass, 1.8mm diameter) are used to collimate the light launched into the subject. The launched light on each path is approximately 7 μW for each wavelength.

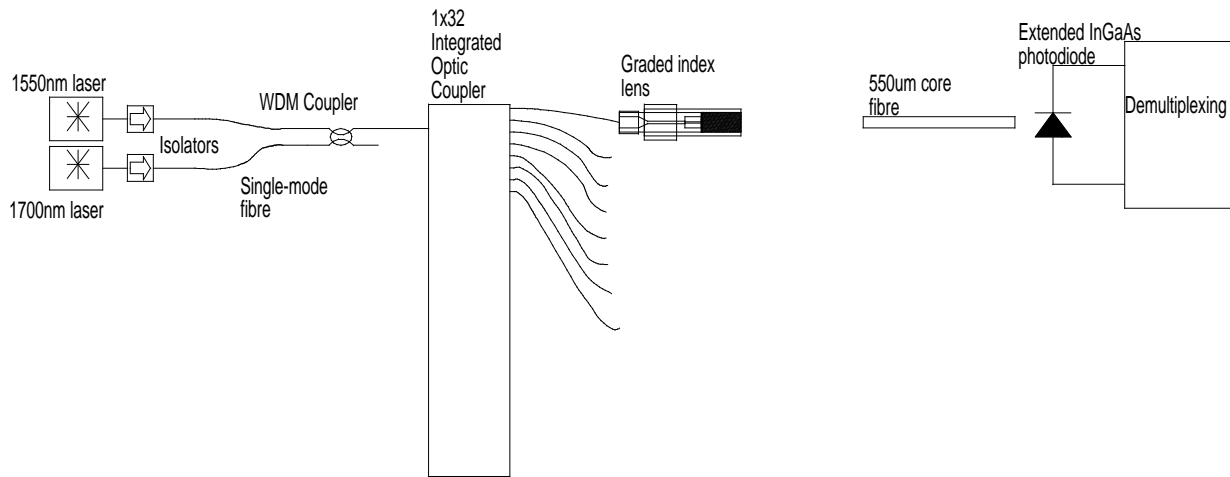


Figure 2 The optical circuit (one path shown).

The transmitted light is collected by a 550µm diameter fibre and detected by an extended InGaAs photodiode (Fermionics FD1000W2.2). The 1550nm and 1700nm signals are encoded by frequency modulation of the sources at 160kHz and 90kHz, respectively, with lock-in detection at the receive electronics. In the present system, the modulation frequency is limited to 250kHz by the front-end amplifier of the detector electronics. The electronics of a single-channel are shown schematically in Figure 3.

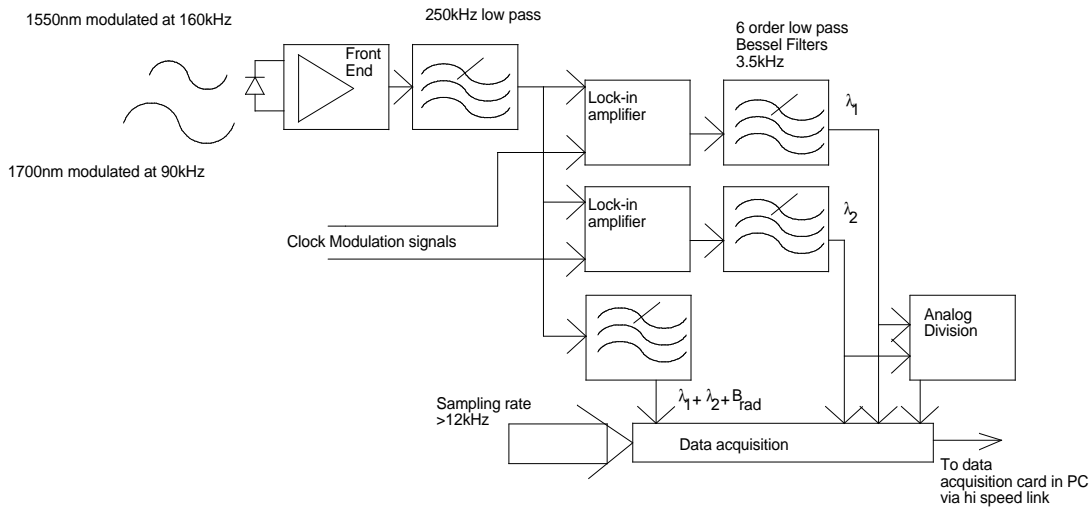


Figure 3 Schematic diagram of a (1 of 32) detector circuit.

2.2. Single-channel performance

In a previous paper³, the feasibility of the measurement approach was demonstrated, and the necessary characteristics of the sources, detectors and optical components were presented. By separating out the received light intensity into signals proportional to the two received wavelengths, it is possible to obtain two signals that in turn enable determination of the path concentration integral of gaseous hydrocarbons:

$$I_r(\lambda_1) = I_o(\lambda_1) \cdot \exp\left(-\int_L k(\lambda_1) c(x, y) dl\right) F \quad I_r(\lambda_2) = I_o(\lambda_2) \cdot \exp\left(-\int_L k(\lambda_2) c(x, y) dl\right) F \quad (3)$$

$$\int_L c(x, y) dl = \frac{1}{k(\lambda_1) - k(\lambda_2)} \ln\left(\frac{I_r(\lambda_2)}{I_r(\lambda_1)} \cdot \frac{I_o(\lambda_1)}{I_o(\lambda_2)}\right) \quad (4)$$

A single channel of the AOE system was used to calibrate the absorption through a 165mm test cell. Figure 4 shows the transmission of 1700.4 nm light through gaseous iso-octane, at an iso-octane concentration of 0.0073 moles/litre, as a function of pressure and temperature. The variation with pressure is significant, with reduced absorption of the laser light as the pressure increases; such a variation is to be expected from pressure broadening of the absorption transition. It is sufficiently well-behaved to provide a simple calibration factor for application to an engine, provided the intra-cycle in-cylinder pressure is recorded simultaneously. The transmission data shown in Fig. 4 with varying temperature show that any effect is very small, and is neglected in the remainder of this paper.

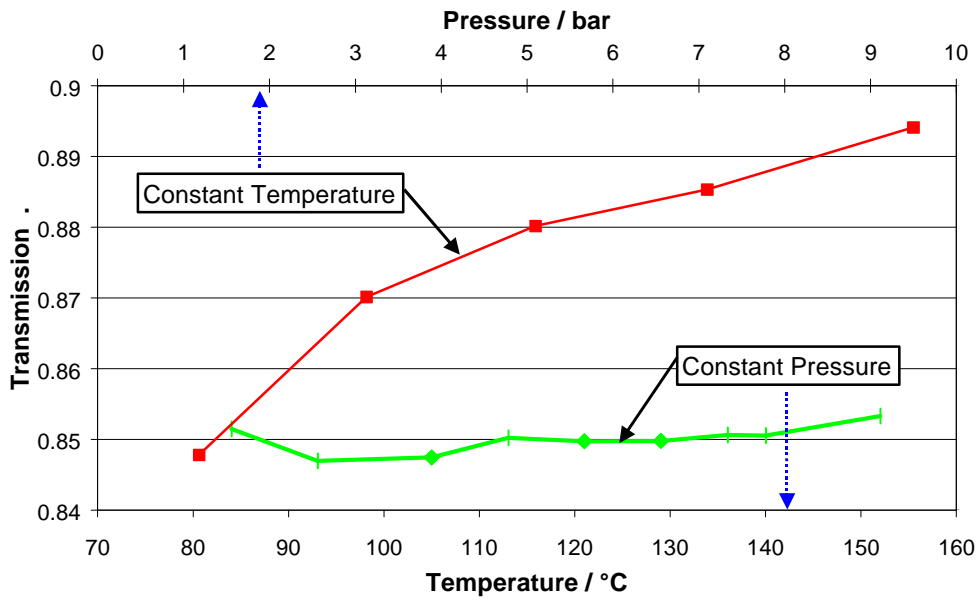


Figure 4 Transmission of iso-octane at 1700.4 nm through a 165 mm test cell as a function of temperature (p= 1 bar) and pressure (T=140°C).

The utility of the dual-wavelength technique is well demonstrated by the results shown in Figure 5, where talcum powder was blown into the light path using compressed air. Whilst the individual light wavelengths show very significant attenuation, with values over 25%, the high degree of correlation between the 1700nm and 1550nm attenuation in this case yields a ratio measurement which is very stable, with measured noise on the ratio being about 50 - 60 dB down, compared with the light signal.

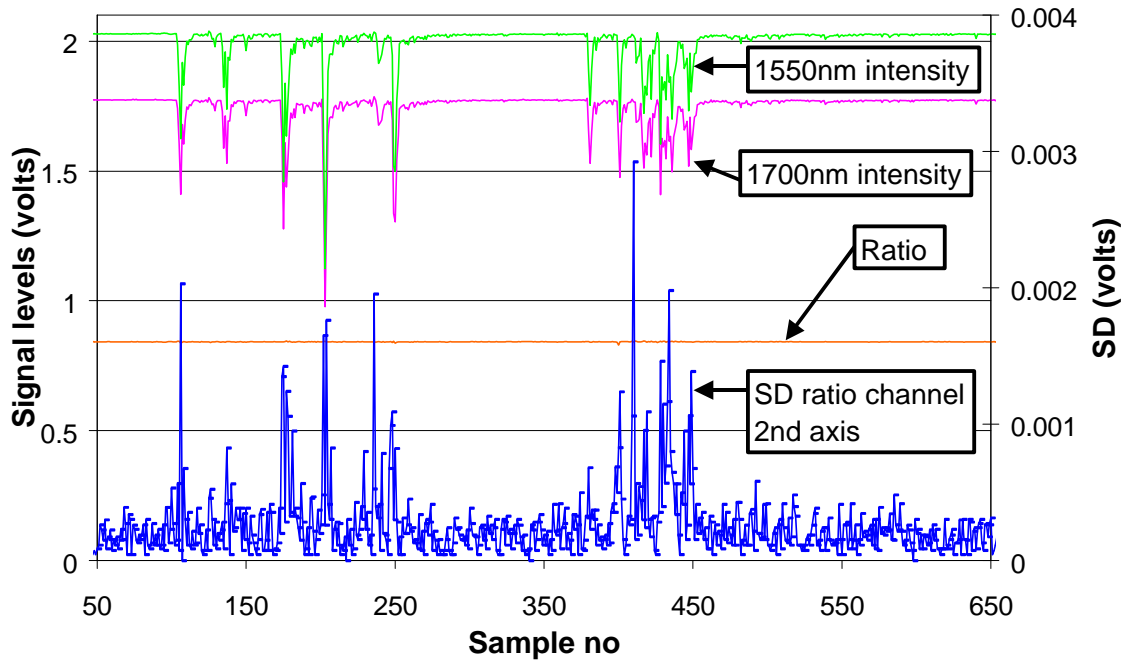


Figure 5 Received light intensities of 1700 nm and 1550 nm light, with particulate clouds being blown into the light path. The ratio signal is shown, and its standard deviation.

In general operation, without any disturbance in the transmission path, the stability of the electronics is excellent, providing noise typically 70dB down compared with the received light intensity. Generally, the true signal-to-noise ratio (considering the absorption as the signal) is a function of absorber concentration and path length. The resolution of small variations of path-integrated concentration values is highly demanding of the electronics. For the 32-channel system, dedicated electronics were built in-house. Analysis and modelling of noise¹⁵ enabled a low-noise system to be developed. The path integrals are measured with a SNR of 28dB for an absorption of 2%. The impact of noise on reconstructed images is critical, see below. The electronic configuration was constrained by the desire to maintain flexibility, e.g. for different photodiode configurations. With a dedicated system, further noise improvements are feasible.

Testing of this single channel on a gas flow of a propane/butane mix showed that, although the refractive index variation causes changes to the path of the lasers through the measurement space, the wavelengths selected displayed negligible differential path deviation. This emphasises the importance of matching the intensity profiles of the measurement and reference lasers^{16,17}.

2.3. Image reconstruction

The system described here is analogous to the so-called "hard-field" X-ray tomographic imaging systems widely used in medicine. Hence, the well-developed image reconstruction techniques for that case^{18,19} can, in principle, be applied here. In practice, the main distinguishing feature of the reconstruction problem faced here is due to the relatively small number of absorption paths through the subject; i.e. the Radon transform is severely under-sampled compared with the case of a typical medical CAT scanner. This implies that the benefit of any physically-motivated regularisation constraints on the reconstructed images could be relatively large. The constraints may be, for example, the requirement that HC concentration in any pixel of the reconstructed image is non-negative, or the use of iterative schemes which attempt to calculate the anticipated path absorption measurements from the current solution of the data inversion, using the Beer-Lambert law. In the work described here, the relative merits of such schemes for our application have not yet been fully explored, and an adaptation²⁰ of the Algebraic Reconstruction Technique (ART)²¹ is used for the images presented in this paper.

In general, the ART technique consists of the solution for \mathbf{C} , the N-vector of concentrations in each of the N pixels in the reconstructed image, in the following equation :

$$\mathbf{A} = \mathbf{WC} \quad (5)$$

where \mathbf{A} is the M-vector of (the natural logarithm of) the measured fractional intensities along all M paths through the subject, and \mathbf{W} is the N x M matrix of weights w_{ij} corresponding to the length of beam j through pixel i. In our case, the reconstruction space was divided into a 100x100 rectangular grid of pixels across which the 4 projections pass. Hence, N = 10,000. However, we have only M = 32 absorption paths, making an analytic solution of equation (6) undetermined, so an iterative approach is adopted. At the start of each iteration synthetic data are produced by solving the forward problem (i.e. using equation (6) to produce a predicted M-vector of measurements \mathbf{A}_s) with the most recent solution for \mathbf{C} . Synthetic and measured data are compared to produce a series of error terms used with the weight matrix to update the pixel concentration values. The entire image is updated by equation (7) on a ray-by-ray basis, q being incremented as each ray is processed. An iteration is complete when all the rays have been treated. The relaxation constant, ω , was set to 0.5 which was found to give reliable stable solutions with a reasonable number of iterations. The convergence is monitored by the magnitude of the relative change of subsequent images from one iteration to the next, as given by equation (8) below, stopping when a value of 0.1% is reached. The iteration number is denoted by p.

$$C_{q+1} = C_q + \frac{\mathbf{w}}{|\mathbf{W}_j|^2} (\mathbf{A}_j - \mathbf{W}_j^T \cdot \mathbf{C}_q) \mathbf{W}_j \quad (6)$$

$$\Delta \text{image} = \frac{\sum_N |C_p - C_{p-1}|}{\sum_N |C_p|} \quad (7)$$

Synthetic data were produced, with various noise levels, to test the sensitivity of the image “pixel noise” to that of the path integral measurements. It was found that, for a stoichiometric iso-octane fuel charge, the precision of the reconstructed pixel concentrations was 0.1 stoichiometry if the measurement SNR was greater than 20dB. For a stoichiometric fuel-air mixture at 10bar, the absorption is typically 2-4%, depending on path length, giving SNR of 28dB or better (see section 2.2).

3. NIR TOMOGRAPHIC IMAGING

To demonstrate the technique in operation by the conventional approaches used in tomography, a phantom would be required in which a static region of gas, containing both HC and air, would reside within a static air host, with no relative movement or diffusion, etc. Clearly, this is impractical, so we have attempted to create various non-stationary phantoms, on which the technique can be demonstrated and explored.

3.1. Single-channel scanning

A simple simulation of an engine combustion chamber was carried out by releasing a gaseous mixture of propane and butane through a 5.5 mm diameter nozzle, to create a laminar flow plume located within an air “host”. A single-channel measurement system (launch and receive) was situated on the edge of the host region and translated/rotated relative to the plume, physically scanning it. The launch-to-receiver distance was 85mm. The 1550/1700 nm power levels in this channel were 50 and 38 μW , respectively. In these experiments, the modulation electronics and lock-in detection were provided by standard laboratory units, prior to construction of dedicated electronics. The experiments were repeated with custom-designed units built in-house. Raw signal-to-noise performance on the detectors was almost identical in both cases, at about 70dB.

The behaviour of the single-channel optical system was studied in detail by relative scanning of the optical path across the plume, making measurements at 0.1mm intervals. Although the general behaviour was as expected, the complex thermodynamic and fluid dynamic system at the edge of the plume demonstrated the need for excellent optical matching of the launch characteristics of the two wavelengths. In the present system, this is exacerbated by the relatively low absorption of 1700nm light by hydrocarbons at combustible concentration in air. Simple corrective measures were implemented, involving laborious alignment procedures.

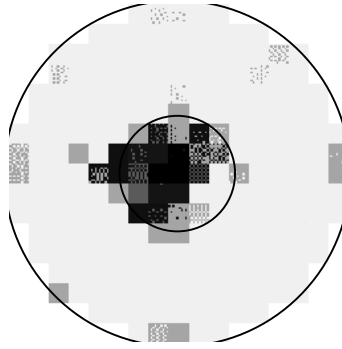


Figure 6 Reconstructed image of HC plume cross-section in a 16 mm diameter host space.

Four projections of the circular region containing the inner part of the host and phantom were obtained by a similar scanning process, each projection containing 33 parallel absorption paths separated by 0.5mm, yielding a total of 132 measurements. Figure 6 shows the reconstructed image of the 16 mm diameter subject. The reconstructed plume, shown in Figure 6, is easily observed and is well located with respect to the actual plume, with an extent which is of similar magnitude to that of the 5.5mm gas outlet.

3.2. Fixed multi-channel operation

The simulation of an IC engine has been attempted by building a sealed chamber, as shown in section 2.1, which is operable at high temperature and pressure, and into which gas is injected at pressure to create a "jet" phantom. The 85mm diameter chamber is sampled by 32 absorption channels in fixed locations with respect to the chamber, as shown in Figure 1. The mode fields of the two wavelengths propagating through the chamber, although coaxial, have slightly different gaussian widths, which is attributed to diffraction in the launch optics (and not due to chromatic aberration, as previously reported²²). This causes a measured 1700/1550nm ratio change as a result of beam deflections due to refractive index variations within the body of gas, which are in turn due to temperature and density variations. The effects of such refractive index variations have been calculated previously, relating to temperature differences within a gas flow²³, and in-cylinder gas concentration measurements have suffered increased noise due to such refractive index variations¹⁶. Several options are available to solve this particular problem in our system, for example, choice of a reference wavelength nearer to that of the absorbed wavelength. For the present purpose, it does not prevent demonstration of the technique.

To allow the testing of a 32-channel system, a pressure vessel with optical access was designed and constructed to simulate the combustion chamber of an engine. The vessel could be operated over 40-250°C temperature and 1-12 bar pressure ranges, comparable to those experienced in a spark ignition engine. Fuel injection was provided either by a Mitsubishi GDI injector in the liquid fuel case (to be reported separately), or by two fast solenoid valves for gaseous fuel (reported here). In the analysis below, averaged absorption data are used for 25 injection events, for the purpose of demonstrating the general plume shape and its development with reduced stochastic variation. Reconstructed data are shown in Fig. 7 for a 20ms injection of gaseous propane, with the measurement plane 10mm below the injector. The location of the injection port is marked and a concentration scale (arbitrary units) is provided, red indicating high concentration and green low. The images shown were recorded at 0, 30, 60, 120 and 240ms after the start of injection. The temporal resolution of the images in this instance is 1.2ms, due to signal averaging.

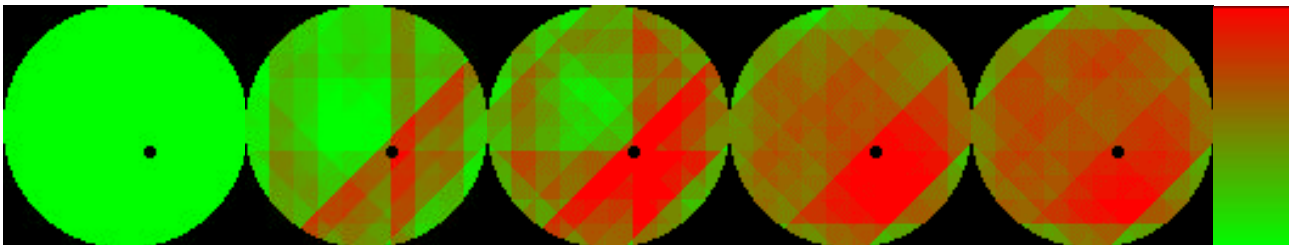


Figure 7 Reconstructed images of propane concentration (10 mm below injector) for a 20 ms gas injection.

Further work on appropriate reconstruction algorithms would yield considerable benefit. Clearly, the restriction to 32 channels causes relatively poor spatial resolution. Nevertheless, the injector location is well identified, and the diffusion of gas over the whole chamber is still not complete after 240ms.

A dual gas-injection experiment was performed to demonstrate the spatial resolution of the system, see Fig. 8. The injectors labelled A and B injected propane for 10ms, but injector B was delayed by 100ms compared with A. The images shown in Fig. 8 are at 0, 94, 138, 192, 552ms. The spatial resolution is clearly better than the injector separation, which is $D/2.8$. The fuel and air is nearly in the well-mixed condition for the image at 552ms.

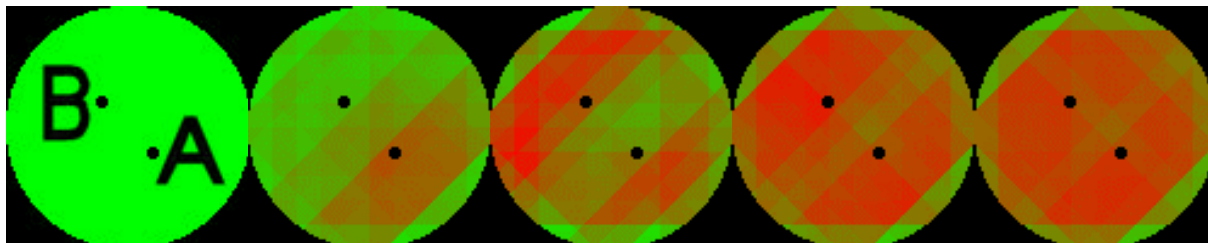


Figure 8 Reconstructed images of propane concentration (10 mm below injector) for dual gas injections.

Further developments of the system could involve the incorporation of embedded lenses into the wall of the pressure vessel²⁴ rather than use of external optics. This would provide greater immunity to pressure changes within the chamber, which currently cause beam deflection at the glass/chamber space boundary. However, for many applications, pressure is known or can be readily compensated for.

4. DISCUSSION

One of the main objectives of the current study has been borne out by the data in Figures 4, 6, 7 and 8, where different HC species are clearly shown to be measurable, in air, by the same 2-wavelength All-Opto-Electronic system. (Note, however, that these different HC species would not be distinguishable if present in the subject simultaneously.) To date, only the iso-octane case has been fully calibrated for the determination of concentration distribution, hence Figures 6, 7 and 8 do not present quantitative concentration "images". However, there is no indication in our work to date that such calibration cannot be readily achieved for propane and propane/butane mixtures.

Despite the relatively low absorption of 1700nm light by combustible concentrations of HC in air, the 2-wavelength technique is clearly capable of providing useful contrast for tomographic imaging of such HC distributions. The excellent pressure and temperature behaviour of absorption in the single-channel data of Figure 4, and the particle immunity demonstrated in Figure 5, are very promising.

The difficulty of producing a simple phantom, without complex fluid flow and thermodynamic behaviour at the interface region between air and HC, is very severe for development and characterisation work. Nevertheless, the image data in Figures 7 and 8 are very encouraging and demonstrate the fundamental promise of the technique.

To the best of our knowledge, Figures 7 and 8 are the first published tomograms showing chemically specific imaging sensitivity using absorption tomography with an AOE system, containing no bulk optical components and no moving parts. This system is also readily applicable to HC gas/gas mixing in other cases where optical access can be achieved.

One design feature, which must be given further attention, is the critical need to ensure that both wavelengths are exposed to the subject with a high level of equivalence in terms of their optical path. Otherwise, thermodynamic and fluid-dynamic influences on the differential signal can be significant. Modified optical configurations of the launch and receive systems will be investigated, as will the use of a closer reference wavelength.

The above feature is exacerbated by the low absorption at 1700nm. We are investigating an approach for HC which concerns optimal tuning around $3.4\mu\text{m}$ to achieve a balance between penetration and absorption signal strength. This would have the added benefit of significantly reduced influences of particulate scattering. However, such a design would imply the

use of more expensive and more complex optical technologies, e.g. chalcogenide fibres, ZnSe lenses, etc. For some applications where no alternative is available, this may be appropriate.

Further improvements of the SNR in the measurement of path concentration are feasible, although the benefit for the image properties remain to be fully analysed.

5. CONCLUSIONS

A 2-wavelength All-Opto-Electronic NIR absorption system has been demonstrated to provide 2-dimensional tomographic images of a chemical species distribution in a mixture of gases. By operating at 1700nm, commercially available opto-electronic components could be used, although the small HC absorption at this wavelength (for short path-length combustible concentrations of HC) places considerable demands on the electronics and optics of the system. Spatial resolution is of the order of $D/5$ as shown by the multiple injections. Temporal resolution is of the order of 1000 frames per second.

In particular, further work is necessary on the optics of the system. However, the robustness of the design to pressure and temperature variation, and to particulates within the subject, are all very promising.

The authors would like to acknowledge EPSRC for the support of this work via grant number GR/L67592, and a CASE studentship (FPH) in conjunction with AVL(UK). The authors are grateful for helpful discussions with Dr Ernst Winklhofer (AVL), Mr Stan Wallace and colleagues (Rover Ltd.) and Dr Steve Nattrass (Shell Research Ltd.).

6. REFERENCES

1. P.J. Holden, M. Wang, R. Mann, F.J. Dickin, R.B. Edwards, *Imaging stirred vessel macromixing using electrical resistance tomography*, *AIChE J.* **44**, pp.780-790, 1998.
2. M.R. Hawksworth and D.J. Parker, in *Process Tomography : Principles, Techniques and Applications* (Eds. R.A. Williams and M.S. Beck), Butterworth-Heinemann , Oxford , 1995.
3. S.J. Carey, H.McCann, F.P. Hindle, K.B. Ozanyan, D.E. Winterbone, E. Clough, *Chemical species tomography by near infra-red absorption*, *Chem. Eng. J.* **77**, pp. 111-118, 2000
4. R. Stone, *Introduction to Internal Combustion Engines*, Macmillan Press Ltd, London, 1999
5. H. Zhao, N. Ladommatos, *Optical Diagnostics for In-cylinder mixture formation measurements in IC engines*, *Prog. Energy Combust Sci.* **24** , pp. 297-336, 1998
6. E Winklhofer, H Fuchs, *Laser induced Fluorescence and flame photography tools in gasoline engine combustion analysis*, *Optics and Lasers in Engineering* **25**, 379-400, 1995.
7. M. Berckmuller, N.P. Tait, D.A. Greenhalgh, *The time history of the mixture formation process in a lean-burn stratified-charge engine*, Society of Automotive Engineers Special Publications, **1212**, 77-99 (SAE 961929), 1996, ISSN 0099-5908.
8. F.P. Hindle, H.McCann and K.B. Ozanyan , *First demonstration of Optical Fluorescence Auto-Projection Tomography*, *Chem. Eng. J.* **77** , pp. 127-135, 2000.
9. U. Spicher et al., *Application of a new optical fibre technique for flame propagation diagnostics in IC engines*, Society of Automotive Engineers Special Publications, **1348**, 1-13 (SAE 980139), 1998.
10. H. Philipp, A. Plimon, G. Fernitz, A. Hirsch, G. Fraidl, E. Winklhofer, *A tomographic camera system for combustion diagnostics in SI engines*, Society of Automotive Engineers Technical Paper Series, SAE 950681, 1-16, 1995, ISSN 0148-7191.
11. S.R. Nattrass, D.M. Thompson, H. McCann, *First in-situ measurement of lubricant degradation in the ring-pack of a running engine*, Society of Automotive Engineers Special Publications, **1055**, 153-165 (SAE 942026), 1994, ISSN 0148-7191.
12. E. Winklhofer, G. Fraidl, A. Plimon, *Monitoring of gasoline fuel distribution in a research engine*, *Proceedings of the Institution of Mechanical Engineers, Part D: Journal of Automobile Engineering*, **206**, 107-115, 1992.

13. H. Kawazoe, K. Inagagi, Y. Emi, F. Yoshino, *Computer tomography measurement of gaseous fuel concentration by infra-red laser light absorption*, SPIE 3172, pp.379-400, 1997
14. S.M. Skippon, S.R. Nattrass, J.S. Kitching, L. Hardiman, H. Millar, *Effects of fuel composition on in-cylinder air/fuel ratio during fuelling transients in an SI engine, measured using differential infra-red absorption*, Society of Automotive Engineers Technical Paper Series, SAE 961204, 1996.
15. S.J. Carey, *Chemical Species Tomography by Near Infra Red Absorption*, PhD Thesis, UMIST, 2001.
16. E. Winklhofer, A. Plimon, *Monitoring of hydrocarbon fuel-air mixtures by means of a light extinction technique in optically accessed research engines*, Optical Engineering 30, pp. 1262-1268, 1991
17. Drallmeier A "Hydrocarbon-vapor measurement in pulsed fuel sprays" *Applied Optics* **33**, 7781-7788, 1994.
18. A.C. Kak, M. Slaney, *Principles of Computerized Tomography*, IEEE Press, New York, 1988
19. F. Natterer, *Mathematics of Computerized Tomography*, J. Wiley and Sons, Stuttgart, 1986.
20. F. P. Hindle, *Absorption and Fluorescence Tomography for Hydrocarbon Distribution Measurement in Internal Combustion Engines*, PhD Thesis, UMIST, 2000.
21. R. Gordon, *A Tutorial on ART (Algebraic Reconstruction Techniques)*, IEEE Trans. on Nuclear Science, NS-21. Pp.78-93, 1974.
22. McCann H, Carey S, Hindle F, Ozanyan K, Winterbone D, Clough E, *Near Infra-Red absorption tomography system for measurement of gaseous hydrocarbon distribution*, SPIE Conference on Process Imaging for Automatic Control, Boston (Nov. 2000), Proc. SPIE **4188**, 141-150.
23. E.J. Beiting, *Fibre-optic fan-beam absorption tomography*, Applied Optics 31, pp. 1328-1343, 1992
24. H. Philipp, G.K. Fraidl, P. Kapus, E. Winklhofer, *Flame Visualisation in Standard SI-Engines - Results of a Tomographic Combustion Analysis*, Society of Automotive Engineers Special Publications, **1244**, 153-162 (SAE970870), 1997, ISSN 1054-6693.